Effects of Amino Acid Replacements on the Reductive Unfolding Kinetics of Pancreatic Trypsin Inhibitor†

Jose A. Mendoza,‡ Michael B. Jarstfer,§ and David P. Goldenberg*

Department of Biology, University of Utah, Salt Lake City, Utah 84112

Received September 2, 1993; Revised Manuscript Received November 16, 1993®

ABSTRACT: In order to characterize the major transition states in the disulfide-coupled folding pathway of bovine pancreatic trypsin inhibitor (BPTI), the reductive unfolding kinetics of wild-type BPTI and 18 variants with single amino acid replacements were measured in the presence of varying concentrations of dithiothreitol (DTT_{SH}^{SH}). As observed previously for the wild-type protein, unfolding of the mutant proteins was found to proceed through the formation of a native-like two-disulfide intermediate (N_{SH}^{SH}), followed by either direct reduction of this intermediate or intramolecular rearrangement to generate other two-disulfide species that were then reduced further. From the dependence of the rate of disappearance of N_{SH}^{SH} on the concentration of DTT_{SH}^{SH}, the rate constants for the direct and rearrangement mechanisms were estimated. All of the amino acid replacements examined were found to increase both rate constants, with some mutants unfolding as much as 10 000-fold more rapidly than the wild-type protein. The two rate constants were highly correlated by a linear free energy relationship, suggesting that the transition states for the direct and rearrangement mechanisms are very similar in their response to amino acid replacements. These results are consistent with a model in which the two transition states, which are also the major transition states for disulfide-coupled refolding, are extensively unfolded.

Bovine pancreatic trypsin inhibitor (BPTI)[1] is a small protein composed of 58 amino acid residues that folds into a well-defined three-dimensional structure stabilized by three disulfide bonds (Figure 1). Its folding pathway has been elucidated by trapping and characterizing disulfide-bonded intermediates (Creighton, 1978, 1990; Creighton & Goldenberg, 1984; Weissman & Kim, 1991; Goldenberg, 1992) and may be summarized schematically as below:

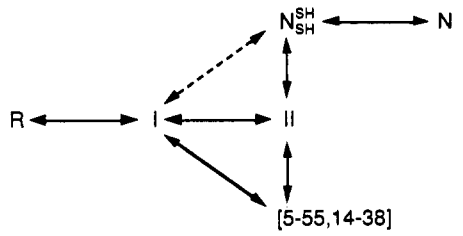

(1)

R and N represent the reduced and unfolded protein and the native state, respectively; I and II are populations of intermediates with one and two disulfide bonds; N_{SH}^{SH} is a native-like intermediate ([30–51,5–55]) that contains two of the three disulfides of the native protein, as is [5–55,14–38]. The population designated here as II is dominated by the third species containing two of the three native disulfides ([30–51,14–38]) but also contains at least two species with nonnative disulfides. The population of one-disulfide intermediates contains about 60% [30–51] and smaller amounts of other species, including [5–55].

One of the striking features of the BPTI folding pathway is that the kinetically preferred mechanism involves intramolecular disulfide rearrangements rather than direct sequential formation of the three disulfide bonds found in the native protein. Although the immediate precursor of the native protein, N_{SH}^{SH}, can be formed directly from the one disulfide intermediates, the rate of the intramolecular step in this reaction, indicated by the dashed line in eq 1, is about 5000-fold lower than for forming the other two-disulfide species (Creighton, 1977a; Goldenberg, 1988). Once these other species form, they must undergo rearrangements to generate N_{SH}^{SH}. The formation of N_{SH}^{SH} must proceed via at least one species with a nonnative disulfide, a role that is likely to be played by the minor components of II ([30–51,5–14] and [30–51,5–38]).

Two of the slowest interconversions during folding are the intramolecular rearrangement between II and N_{SH}^{SH} and the direct formation of N_{SH}^{SH} from the one-disulfide intermediates. The reverse of these reactions are also very slow, making N_{SH}^{SH}, which is active as a trypsin inhibitor, kinetically very stable. In the presence of 1–50 mM reduced dithiothreitol (DTT_{SH}^{SH}), the reductive unfolding of N_{SH}^{SH} has a half-time of about 20 h at 25 °C, pH 8.7 (Creighton, 1977b; Goldenberg, 1988). Thus, the high transition-state energies of these two steps in the BPTI folding pathway have important implications for both the mechanism of folding and the kinetic stability of the folded conformation.

† Supported by NIH Grant GM42494.

* To whom correspondence should be addressed.

‡ Present address: Department of Biochemistry, University of Texas Health Science Center at San Antonio, 7703 Floyd Curl Drive, San Antonio, TX 78284-7760

§ Present address: Department of Chemistry, University of Utah, Salt Lake City, UT 84112.

® Abstract published in *Advance ACS Abstracts,* January 15, 1994.

[1] Abbreviations: BPTI, bovine pancreatic trypsin inhibitor; the disulfides of native BPTI and folding intermediates are indicated by the residue numbers of the disulfide-bonded cysteine residues; N_{SH}^{SH}, native-like two-disulfide intermediate containing the 30–51 and 5–55 disulfides; other intermediates are indicated by the disulfide bonds they contain; amino acid replacements are indicated by the wild-type residue type (using the one-letter code for the 20 standard amino acids), followed by the residue number and the mutant residue type; DTT_S^S and DTT_{SH}^{SH}, disulfide and dithiol forms of dithiothreitol; Tris-HCl, tris(hydroxymethyl)aminomethane hydrochloride; EDTA, ethylenediaminetetraacetic acid; HPLC, high-performance liquid chromatography.

0006-2960/94/0433-1143$04.50/0

The intramolecular rate constants for forming N_{SH}^{SH} via the two mechanisms are quite similar, leading Creighton (1978) to suggest that they might involve similar conformational transitions. In the folding of two BPTI homologues, however, the intramolecular rate constant for the direct formation of N_{SH}^{SH} is substantially faster than that for the rearrangement reaction, suggesting that the conformational changes required for the two processes may not be identical (Hollecker & Creighton, 1983; Goldenberg & Creighton, 1985). Weissman and Kim (1992) have directly measured the rates at which the minor nonnative components of II, [30–51,5–14] and [30–51,5–38], undergo intramolecular rearrangements and have found that these species rearrange to produce either N_{SH}^{SH} or [5–55,14–38] at similar rates, suggesting that the rearrangements are random processes involving extensive unfolding of structure present in the intermediates.

In order to characterize further the transition states for the direct reduction and rearrangement of N_{SH}^{SH}, we have examined the effects of single amino acid replacements on the kinetics of unfolding. Because the reductive unfolding of BPTI does not require elevated temperature or the addition of denaturants, folding and unfolding kinetics can be measured under conditions that are identical except for the concentrations of thiol and disulfide reagents. The transition states characterized in folding and unfolding experiments are thus expected to be equivalent.

As described previously, mutations in the BPTI gene have been isolated by screening randomly mutagenized clones to identify those that produce proteins that can fold to the native conformation but are inactivated much more rapidly than the wild-type protein when treated with DTT_{SH}^{SH} (Coplen et al., 1990). Initial characterization of 18 of these "DTT-sensitive" mutants, as well as 12 site-directed mutants with a similar phenotype, demonstrated that many, but not all, of these mutants unfold much more rapidly than the wild-type protein (Goldenberg et al., 1992). All of the substitutions leading to rapid unfolding (i.e., half-times of 3 min or less) are located in the region of the native protein that includes the two disulfides that are reduced most slowly during the unfolding of the wild-type protein. These results indicated that the kinetic stability of N_{SH}^{SH} is primarily determined by interactions within the portion of the folded protein including the C-terminal α-helix and most of the β-sheet. However, these preliminary experiments did not indicate whether the mutations that increase the rate of unfolding do so by accelerating the direct reduction of N_{SH}^{SH} or its rearrangement, or both.

In the present study we have examined in greater detail the unfolding kinetics of 18 BPTI variants, with amino acid replacements at 13 of the 58 residues of the wild-type protein. For each of the mutant proteins, the kinetics of unfolding were measured as a function of DTT_{SH}^{SH} concentration, so as to distinguish between the rearrangement mechanism, which is expected to be independent of reductant concentration, and the direct reduction reaction, with a rate proportional to DTT_{SH}^{SH} concentration. These measurements indicate that all of the substitutions examined enhance the rates of the two mechanisms in a nearly parallel fashion, suggesting that the transition states for the two processes are very similar.

EXPERIMENTAL PROCEDURES

Preparation of Mutant Proteins. BPTI variants were produced in *Escherichia coli* HB101 harboring plasmids in which the mutant BPTI genes were fused to a sequence encoding the signal peptide of the *E. coli* Omp A protein (Goldenberg, 1988). In these strains, the signal peptide is removed, and the BPTI produced is correctly folded. Bacterial cultures were grown at 30 °C in supplemented minimal medium, as described previously (Coplen et al., 1990). For each variant, the BPTI from a 500-mL culture was purified by ion exchange (CM-Trisacryl M, IBF Biotechnics), gel filtration (Sephadex G-50), and reversed-phase HPLC (Vydac C_{18}) chromatography as described previously (Goldenberg et al., 1992, 1993). The BPTI samples were estimated by gel electrophoresis to be more than 95% pure.

Table 1: Rate Constants for Rearrangement and Direct Reduction of N_{SH}^{SH}

	rearrangement		direct reduction	
variant	k_{rearr} (s^{-1})	% error[a]	k_{dir} (s^{-1} M^{-1})	% error[a]
wild type	3.0×10^{-6}	2	8.4×10^{-5}	5
P2A	3.0×10^{-4}	6	2.9×10^{-2}	24
P9L	6.4×10^{-4}	10	5.2×10^{-2}	31
G12A	2.6×10^{-5}	11	2.3×10^{-3}	22
Y21L	2.5×10^{-4}	10	1.8×10^{-2}	13
Y21N[b]	2.3×10^{-3}	11	1.4×10^{-1}	31
F22I[b]	2.5×10^{-3}	13	3.0×10^{-1}	19
F22L[b]	2.8×10^{-3}	16	2.3×10^{-1}	33
Y23L	2.4×10^{-2}	70	1.5×10^{1}	19
Y23S[b]	1.8×10^{-2}	7	6.6	6
N24P[b]	1.1×10^{-2}	4	3.2	2
G28V	5.9×10^{-5}	43	6.8×10^{-3}	32
L29P[b]	7.0×10^{-3}	37	3.0	15
F33A	6.9×10^{-4}	13	5.7×10^{-2}	28
Y35L	1.8×10^{-4}	10	9.5×10^{-3}	18
N43A	1.2×10^{-2}	7	1.0	8
N43G	4.1×10^{-3}	15	6.7×10^{-1}	16
F45L[b]	3.3×10^{-2}	7	9.8	8
F45S[b]	4.9×10^{-2}	16	5.1×10^{1}	50

[a] The estimates of error reported were obtained from the linear regression of k_{app2} versus DTT_{SH}^{SH} concentration, as in Figure 3. [b] These variants were isolated as "DTT-sensitive" mutants in a screen of randomly mutagenized clones and were previously shown to unfold with half-times of 3 min or less in the presence of 1 mM DTT at pH 8.7, 25 °C (Goldenberg et al., 1992). The other mutants were constructed by oligonucleotide directed mutagenesis, as described previously (Goldenberg et al., 1989, 1992).

Unfolding Kinetics. Unfolding reactions were carried out at 25 °C in the presence of 0.1 M Tris-HCl, pH 8.0, 0.2 M KCl, 1 mM EDTA, and various concentrations of DTT_{SH}^{SH}. The protein concentration was 30 μM. All of the reactions were carried out under an N_2 atmosphere in septum vials. At various time intervals after the initiation of unfolding by the addition of DTT_{SH}^{SH}, samples were withdrawn and reacted with sodium iodoacetate (0.1 M, final concentration) to block any free thiols. The trapped species were separated by electrophoresis through nondenaturing polyacrylamide gels, and the protein bands were visualized by staining with Coomassie blue. The relative concentrations of the species trapped at various times were estimated by video densitometry (Goldenberg et al., 1993).

RESULTS

The 18 BPTI variants examined in this study are listed in Table 1, and the sites of the substitutions in the protein's three-dimensional structure are illustrated in Figure 1. Eight of the mutants examined were isolated in the screen for DTT-sensitive mutants, while the other 10 were constructed by oligonucleotide-directed mutagenesis. The mutations examined cause a variety of substitutions throughout the protein, but the majority of sites chosen for this study are located in the central β-sheet of the protein, since previous results

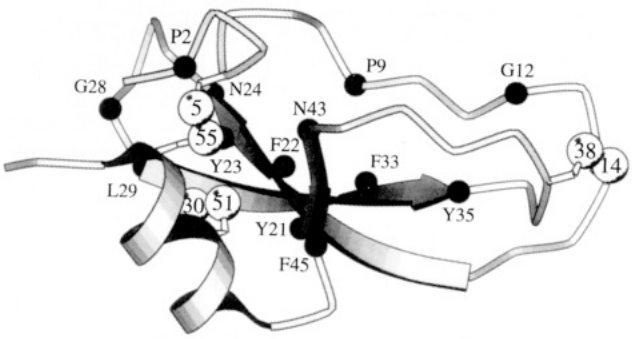

FIGURE 1: Three-dimensional structure of wild-type native BPTI, drawn from the coordinates of the form II crystal (Wlodawer et al., 1987; 5PTI in the Brookhaven Protein Data Bank) with the program MOLSCRIPT (Kraulis, 1991). Positions of the amino acid replacements used in this study are indicated by filled circles.

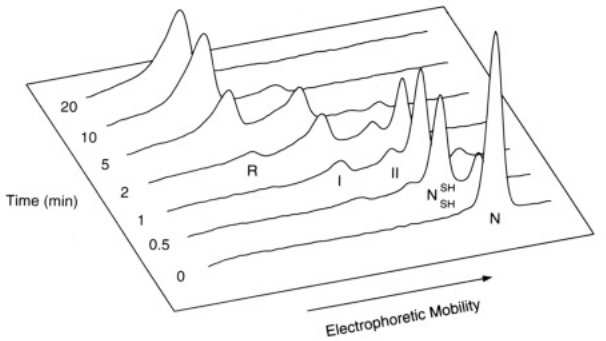

FIGURE 2: Gel electrophoresis profiles of intermediates trapped in the unfolding of the native form of the N43A BPTI variant. The protein was incubated at pH 8.0, 25 °C, in the presence of 0.5 mM reduced DTT to promote unfolding. At the indicated times, samples were withdrawn and reacted with sodium iodoacetate, and the samples were analyzed by nondenaturing gel electrophoresis. The Coomassie-blue stained gels were scanned with a video densitometer to generate the profiles. The mobilities of the native protein (N), the native-like two disulfide intermediate N_{SH}^{SH}, a population of intermediates with two disulfide bonds (II), a population of intermediates with one disulfide bond (I), and the reduced form (R) of BPTI are indicated.

implicated this region as playing the major role in establishing the kinetic stability of the folded protein (Goldenberg et al., 1992). All of the proteins inhibit trypsin stoichiometrically at micromolar concentrations.

The reductive unfolding kinetics of the mutant proteins were measured using techniques and conditions similar to those used previously to study wild-type and other mutant forms of BPTI (Creighton & Goldenberg, 1984; Goldenberg et al., 1989, 1992). To initiate unfolding, native protein was mixed with DTT_{SH}^{SH} and incubated at pH 8.0, 25 °C. At various times after the addition of DTT_{SH}^{SH}, samples were withdrawn and mixed with sodium iodoacetate to irreversibly block any free thiols. The trapped proteins were then fractionated by nondenaturing gel electrophoresis (Figure 2). Under the electrophoresis conditions used, species with fewer disulfide bonds migrate more slowly because they are less compact and because the net positive charge of the protein is decreased by the reaction of the free Cys thiols with iodoacetate.

Figure 2 illustrates the electrophoretic profiles obtained for samples trapped during the unfolding of N43A BPTI with 0.5 mM DTT. As in the unfolding of the wild-type protein, the initial product of reduction of the mutant proteins was a species with a mobility slightly less than that of the native protein. Comparison with the electrophoretic mobilities of the well-characterized wild-type BPTI intermediates indicates that this species has two disulfide bonds and a native-like conformation. Although the identity of the initial reduction intermediate has not been determined directly for most of the mutant proteins, its electrophoretic mobility and kinetic behavior indicate that it is almost certainly N_{SH}^{SH}, the species in which the 14–38 disulfide is reduced. This intermediate was then converted to other intermediates with two (II) or one (I) disulfides and, finally, the fully reduced protein. The major qualitative differences observed among the protein variants were the times required for complete unfolding, which varied from 5 to 6000 min, and the levels to which the intermediate populations I and II accumulated. In general, significant accumulations of I and II were observed only with those mutants for which the half-time of disappearance of N_{SH}^{SH} was less than about 20 min.

In order to determine the rate constants for the direct reduction of N_{SH}^{SH} and its intramolecular rearrangement, the kinetics of reduction were measured at various DTT_{SH}^{SH} concentrations, typically ranging from 0.5 to 10 mM. In analyzing the data, the reduction of the native protein and N_{SH}^{SH} were assumed to proceed by the following mechanism:

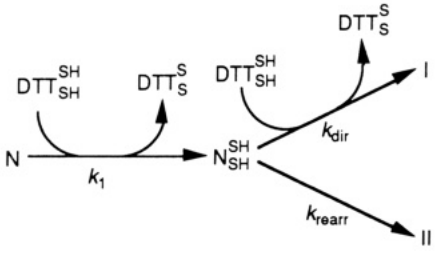

(2)

To facilitate the analysis, a simplified scheme composed of two sequential pseudo-first-order reactions

$$N \xrightarrow[k_{app1}]{} N_{SH}^{SH} \xrightarrow[k_{app2}]{} (II + I) \tag{3}$$

with apparent rate constants

$$k_{app1} = k_1[DTT_{SH}^{SH}] \tag{4}$$

$$k_{app2} = k_{dir}[DTT_{SH}^{SH}] + k_{rearr} \tag{5}$$

was used. For each DTT_{SH}^{SH} concentration, k_{app1} was estimated by fitting the observed time-dependent disappearance of N to the integrated first-order rate expression

$$f_N = e^{-k_{app1}t} \tag{6}$$

where f_N is the fraction of initial protein remaining in the native state at time t. The values of k_{app1} obtained from a direct nonlinear least-squares fit to eq 6 were then used to estimate k_1.

The pseudo-first-order rate constants for the net disappearance of N_{SH}^{SH} were estimated by fitting the observed concentrations of N_{SH}^{SH} to the following integrated rate expression

$$f_{N_{SH}^{SH}} = \frac{k_{app1}}{k_{app2} - k_{app1}}[e^{-k_{app1}t} - e^{-k_{app2}t}] \tag{7}$$

where $f_{N_{SH}^{SH}}$ is the fraction of the total protein with the first disulfide reduced. For each mutant, the average value of k_1, estimated as described above, was used to calculate k_{app1} for each DTT_{SH}^{SH} concentration. The observed values of $f_{N_{SH}^{SH}}$ were fit to eq 7 by nonlinear least-squares with k_{app2} as the only adjustable parameter. Examples of the fit to the experimental data for the N43G variant are illustrated by the dashed lines

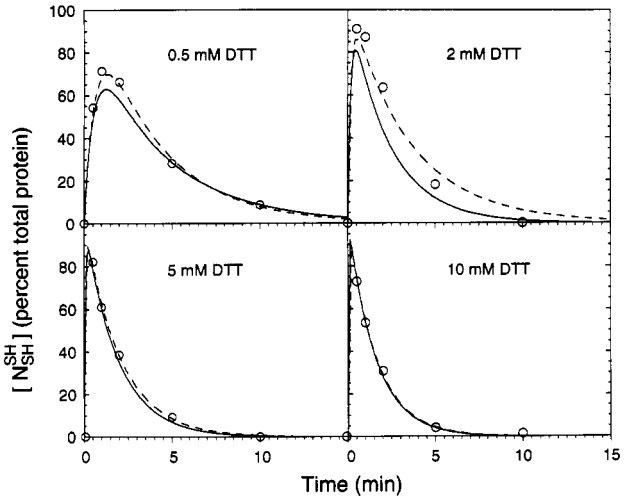

FIGURE 3: Time course of appearance and disappearance of the native-like intermediate, N_{SH}^{SH}, in the reductive unfolding of the N43G BPTI variant in the presence of various concentrations of DTT_{SH}^{SH} at 25 °C and pH 8.0. The open circles indicate the observed concentrations of N_{SH}^{SH}, expressed as the fraction of total protein. The dashed lines are the curves fit to the individual data sets using the simplified first-order kinetic model (eq 7). The solid lines are those generated by complete simulations using a single set of rate constants for all the DTT_{SH}^{SH} concentrations.

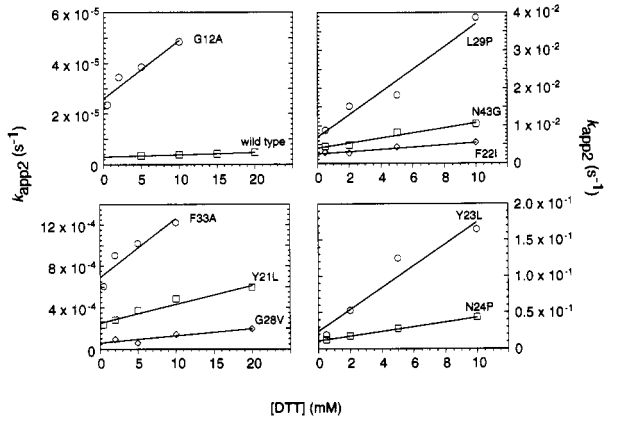

FIGURE 4: Apparent rate constant (k_{app2}) for the disappearance of N_{SH}^{SH} as a function of DTT_{SH}^{SH} concentration. The pseudo-first-order rate constants were obtained by fitting the data obtained at each DTT_{SH}^{SH} concentration to eq 7, as illustrated in Figure 3.

of Figure 3. By this procedure, values of k_{app2} were determined for each DTT_{SH}^{SH} concentration.

To estimate k_{dir} and k_{rearr} for each mutant, k_{app2} was plotted as a function of DTT_{SH}^{SH} concentration, as illustrated in Figure 4. The y-intercept of such a plot is expected to represent the rate constant for the disappearance of N_{SH}^{SH} via mechanisms that are independent of DTT_{SH}^{SH} concentration, i.e., k_{rearr}, while the slope represents the rate constant for the DTT_{SH}^{SH}-dependent process, k_{dir}. For each variant examined, the plot of k_{app2} versus [DTT_{SH}^{SH}] displayed a clear positive intercept and a substantial increase over the range of DTT_{SH}^{SH} concentrations examined, indicating that both rearrangement and direct reduction mechanisms contributed significantly to the net disappearance of N_{SH}^{SH}. Values of k_{rearr} and k_{dir} were determined by least-squares fits of the data (excluding data corresponding to DTT_{SH}^{SH} concentrations less than 0.5 mM) and are listed in Table 1.

To ensure that the assumption of pseudo-first-order kinetics did not lead to spurious results, the rate constants estimated

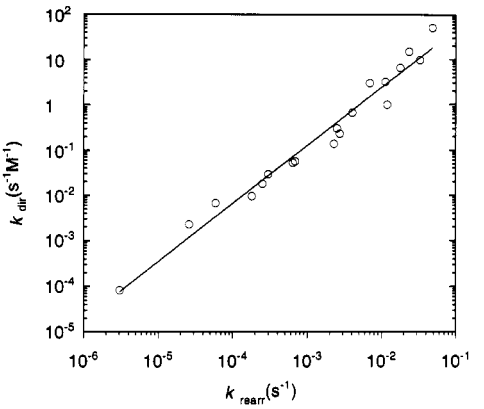

FIGURE 5: Rate constant for direct reduction of N_{SH}^{SH} (k_{dir}) versus the rate constant for intramolecular rearrangement of this species (k_{rearr}) for different BPTI variants. The line represents the equation $\log(k_{dir}) = 1.3 \log(k_{rearr}) + 2.9$.

in this way were tested by numerically integrating the rate expressions representing the full unfolding–refolding mechanism (Creighton & Goldenberg, 1984). In these simulations, the changes in concentration of all of the species, including DTT_{SH}^{SH} and DTT_{S}^{S}, were incorporated. The solid lines in Figure 3 represent the results of such simulations for the N43G variant, using the values of k_{rearr} and k_{dir} from Table 1. Similar consistency between the experimental data, the simplified pseudo-first-order mechanism, and complete simulation was observed for the other variants examined.

The values of both k_{rearr} and k_{dir} were found to vary over a wide range, with k_{rearr} varying from 3.0×10^{-6} s^{-1} for the wild-type protein to 4.2×10^{-2} s^{-1} for the F45S variant, and k_{dir} ranging from 8.4×10^{-5} to 51 s^{-1} M^{-1} for the wild-type and F45S proteins, respectively. In addition, the two rate constants were found to be closely correlated, as illustrated in Figure 5, where the two are plotted on logarithmic scales. This correlation is particularly striking in view of the many different types of amino acid replacements examined here. Some of the replacements represent the deletion of only a few atoms and may cause minimal structural perturbations, while others, such as those that introduce Pro residues or replace Gly residues at sites where the backbone conformation of the wild-type protein is incompatible with these changes, almost certainly lead to local changes in the structure of the native protein.

It is possible, though we believe unlikely, that the correlation observed between the two rate constants could arise from an artifact of the analysis. The experiments described here were not sufficient to determine all of the rate constants in the unfolding–refolding mechanism, and it is conceivable that the observed dependence of the apparent rates on the concentration of DTT_{SH}^{SH} could arise from the reduction steps following the rearrangement of N_{SH}^{SH}, rather than the direct reduction of this species. This could occur if the reduction steps following the rearrangement were not rapid enough to make the rearrangement essentially irreversible. To rule out this possibility, the rates of direct reduction of N_{SH}^{SH} for several mutants have been measured more directly using chemically modified proteins in which the 14–38 disulfide was selectively reduced and alkylated (J. X. Zhang and D. P. Goldenberg, unpublished results). A total of eight variants have been examined in this way, and the rate constants for direct reduction of the blocked proteins, which varied from 5×10^{-3} to 11 s^{-1} M^{-1} at pH 8.7, were found to be very similar to those determined as described here (after correcting for the

difference in pH) and displayed a similar correlation with the rate constants for rearrangement.

Since the logarithms of the rate constants are proportional to the free energy differences between the ground state (i.e., N_{SH}^{SH}) and the transition states for the two processes, the correlation illustrated in Figure 5 implies a linear free-energy relationship between the two transition states. These results suggest that the two transition states are very similar in their response to amino acid replacements, as discussed further below.

DISCUSSION

The results of previous studies had indicated that many of the amino acid replacements examined here cause large increases in the rate of reductive unfolding of BPTI (Coplen et al., 1990; Goldenberg et al., 1992). The initial characterization of the mutants was not sufficient to determine whether all of the mutations accelerate unfolding by the same mechanism, however. Given the variety of different types of replacements, it might have been expected that some would preferentially increase the rate of direct reduction of N_{SH}^{SH}, perhaps by increasing accessibility of the buried disulfides to the reducing agent, while others might act primarily by favoring rearrangement. The results of the present study indicate that all of the substitutions examined increase both rates in a highly correlated fashion. This correlation suggests that all of the amino acid replacements act in very similar ways and provides new information about the nature of the transition states for the unfolding of N_{SH}^{SH} and its formation during folding.

Although mutations might have a variety of effects on the free energies of N_{SH}^{SH} and the transition states for rearrangement and direct reduction, the results presented here can be largely accounted for by a simple model in which the changes destabilize N_{SH}^{SH} with respect to the transition states by disrupting or weakening interactions that are normally present in N_{SH}^{SH} but broken in the transition states. Consistent with this interpretation, the largest rate increases were those arising from substitutions that alter buried residues in the vicinity of the two disulfides present in N_{SH}^{SH}. There is some indication, however, that the effects of the mutations may be more complicated. If the amino acid replacements were to act solely by destabilizing N_{SH}^{SH}, the slope of the logarithmic plot of k_{dir} versus k_{rearr} would be unity. The observed slope, however, is 1.3 (±0.05), reflecting a preferential increase in the rate of the direct reduction reaction. This pattern might indicate that there is a second mechanism, in addition to complete unfolding, leading to direct reduction that becomes more significant as the protein becomes more destabilized. Alternatively, it is possible that the interactions affected by the mutations are more completely disrupted in the transition state for direct unfolding than in the rearrangement transition state. None-the-less, it seems most likely that the primary effects of the mutations on the two reactions are very similar and reflect features of the transition states that are common to the two reactions.

Since the two disulfides present in N_{SH}^{SH} are completely buried, direct reduction of this species must involve at least partial unfolding. As noted earlier by Creighton (1977a), the rearrangement mechanism, in which the thiol of Cys 14 or 38 attacks one of the buried disulfides, must also involve disruption of at least some structure. In principle, however, each of these processes might involve only partial unfolding, and the regions of N_{SH}^{SH} that are disrupted could be different in the two reactions. If this were the case, some amino acid replacements would be expected to selectively enhance one rate or the other. A substitution that weakens the structure of N_{SH}^{SH} at a site that is unfolded during the rearrangement process but remains in a native-like environment during direct reduction, for instance, would be expected to selectively enhance the rate of rearrangement. The high degree of correlation observed between k_{rearr} and k_{dir} suggests that, in fact, the two transition states are very similar to one another. The pattern can be most easily accounted for if both transition states are extensively unfolded.

If, as suggested above, direct reduction of N_{SH}^{SH} requires complete unfolding, the observed rate constant for this reaction is expected to equal the product of the fraction of time that the protein is unfolded with its disulfides intact and the rate constant for reducing either of two fully exposed disulfides. The fraction unfolded can be estimated from the conformational stabilities of analogs of N_{SH}^{SH} in which Cys 14 and 38 are either chemically blocked or replaced by mutation. For a derivative in which the Cys 14 and 38 thiols are carboxyamidomethylated, the free energy change for unfolding (without breaking the two remaining disulfides) has been determined to be 5.6 kcal/mol at 25 °C, pH 5 (Schwarz et al., 1987), while that determined for a genetically engineered form in which Cys 14 and 38 were replaced with Ala is 6.9 kcal/mol at 15 °C, pH 7.8 (Hurle et al., 1990). These values suggest that the fraction unfolded at 25 °C would be in the range of 8×10^{-6} to 7×10^{-5}. The rate constant for reducing the disulfide of oxidized glutathione with DTT_{SH}^{SH} is about 8 s^{-1} M^{-1} at pH 8.0 (Rothwarf & Scheraga, 1992). Thus, the predicted rate constant for reducing N_{SH}^{SH} via a completely unfolded transition state is in the range of 10^{-4}–10^{-3} s^{-1} M^{-1}, in good agreement with the measured value of 8.4×10^{-5} s^{-1} M^{-1}.

There is also additional mutational evidence suggesting that the transition state for rearrangement is extensively unfolded. Among the wild-type protein and 12 mutants for which all of the forward and reverse rate constants in the folding mechanism have been measured, the free energy difference between the fully reduced and unfolded protein and the transition state for the rearrangement of II to N_{SH}^{SH} varies by less than 1 kcal/mol, while the mutations destabilize the native protein by as much as 7 kcal/mol (Goldenberg et al., 1989; J. X. Zhang and D. P. Goldenberg, unpublished results). This pattern suggests that the rearrangement transition-state resembles the reduced protein much more than it does the native protein. This interpretation is also supported by the observation that the addition of urea stabilizes the transition state with respect to the native-like intermediate [30–51,14–38] (Weissman & Kim, 1991).

The two transition states characterized here are also associated with the slowest steps in the refolding of BPTI. The high energy of the transition state for the direct formation of N_{SH}^{SH} plays a particularly important role in defining the pathway because it is the unusually low rate of this disulfide-formation step that leads to the predominant role of intramolecular rearrangements. High-resolution NMR studies of analogs of the major one-disulfide intermediate, [30–51], indicate that this species contains about two-thirds of the folded structure of the native protein, including the central β-sheet and α-helix (Oas & Kim, 1988; van Mierlo et al., 1992, 1993). If, as suggested by the present studies, the transition state for directly forming N_{SH}^{SH} is largely devoid of stabilizing noncovalent interactions, then it is likely that the structure present in [30–51] would have to be disrupted during this reaction.

Similarly, the other significant one disulfide intermediate, [5–55], is known to have a fully native-like conformation that would have to be extensively unfolded in order to form N_{SH}^{SH} directly (van Mierlo et al., 1991; Staley & Kim, 1992). Because direct formation of N_{SH}^{SH} is so slow, other two-disulfide intermediates (II in eq 1), with varying degrees of native-like structure, form preferentially and must then undergo intramolecular rearrangements to yield N_{SH}^{SH}. These rearrangements represent the reverse of the rearrangement of N_{SH}^{SH} that occurs during unfolding and are likely to involve extensive destabilization of the structure present in the two-disulfide intermediates. Thus, the low rates associated with both mechanisms for forming N_{SH}^{SH} during folding may arise, at least in part, from the need to disrupt stabilizing interactions present in earlier intermediates.

Although the mutational results may be most easily visualized by a model in which the two transition states are fully unfolded, it is also possible that these transition states do contain residual structure but the stability of this structure is simply much less sensitive to the perturbations of amino acid replacements than is N_{SH}^{SH}. This might occur if the structure in the transition states were much more flexible and less cooperative than in a fully folded protein, as suggested in the "protein melting" model of Shakhnovich and Finkelstein (1989).

Analyses of the transition states for other protein unfolding–refolding reactions have generally led to a picture in which the transition state has some properties of the native protein and some of the unfolded state. Many destabilizing amino acid replacements affect primarily the kinetics of unfolding, rather than refolding (Beasty et al., 1986; Perry et al., 1987; Klemm et al., 1991; Chen et al., 1992), consistent with models for unfolding in which multiple interactions must be cooperatively disrupted as the transition state is formed during unfolding. There is, however, evidence for regions of native-like structure in the transition states for some proteins, as detected by mutational effects or ligand binding (Kuwajima et al., 1989; Sancho et al., 1991; Serrano et al., 1992). The effects of temperature and denaturants on unfolding–refolding kinetics indicate that the transition state has a heat capacity similar to that of the native protein, but a degree of solvent exposure intermediate between that of the folded and unfolded states (Tanford, 1968; Segawa & Sugihara, 1984; Kuwajima et al., 1989; Creighton, 1990). At present, the transition states associated with direct reduction or rearrangement of N_{SH}^{SH} appear to be native-like only in the sense that they are constrained by two of the disulfides found in the native protein, one of which is undergoing a thiol–disulfide exchange reaction. It is possible, however, that structure in these transition states may be identified by other probes. On the other hand, it may be the case that the steric constraints imposed by the disulfides require a greater degree of unfolding than for the transition states associated with folding reactions that do not involve the formation or rearrangement of buried disulfides.

In summary, these results indicate that both mechanisms by which N_{SH}^{SH} is unfolded involve extensive disruption of the native-like interactions present in this species. These results are consistent with earlier suggestions that the two transition states are conformationally similar and that their high energies are associated with the stability of the folded conformation (Creighton, 1978; Goldenberg & Creighton, 1985; Weissman & Kim 1992). It remains uncertain whether some residual noncooperative structure may be present in the transition states.

ACKNOWLEDGMENT

We thank Jian-Xin Zhang for sharing his unpublished results and for numerous helpful discussions and David Blair for helpful discussions.

REFERENCES

Beasty, A. M., Hurle, M. R., Manz, J. T., Stackhouse, T., Onuffer, J. J., & Matthews, C. R. (1986) *Biochemistry 25*, 2965–2974.
Chen, B. L., Baase, W. A., Nicholson, H., & Schellman, J. A. (1992) *Biochemistry 31*, 1464–1476.
Coplen, L. J., Frieden, R. W., & Goldenberg, D. P. (1990) *Proteins: Struct., Funct., Genet. 7*, 16–31.
Creighton, T. E. (1977a) *J. Mol. Biol. 113*, 275–293.
Creighton, T. E. (1977b) *J. Mol. Biol. 113*, 295–312.
Creighton, T. E. (1978) *Prog. Biophys. Mol. Biol. 22*, 221–298.
Creighton, T. E. (1990) *Biochem. J. 270*, 1–16.
Creighton, T. E., & Goldenberg, D. P. (1984) *J. Mol. Biol. 179*, 497–526.
Goldenberg, D. P. (1988) *Biochemistry 27*, 2481–2489.
Goldenberg, D. P. (1992) *Trends Biochem. Sci. 17*, 257–261.
Goldenberg, D. P., & Creighton, T. E. (1985) *Biopolymers 24*, 167–182.
Goldenberg, D. P., Frieden, R. W., Haack, J. A., & Morrison, T. B. (1989) *Nature 338*, 127–132.
Goldenberg, D. P., Berger, J. M., Laheru, D. A., Wooden, S., & Zhang, J. X. (1992) *Proc. Natl. Acad. Sci. U.S.A. 89*, 5083–5087.
Goldenberg, D. P., Bekeart, L. S., Laheru, D. A., & Zhou, J. D. (1993) *Biochemistry 32*, 2835–44.
Hollecker, M., & Creighton, T. E. (1983) *J. Mol. Biol. 168*, 409–437.
Hurle, M. R., Marks, C. B., Kosen, P. A., Anderson, S., & Kuntz, I. D. (1990) *Biochemistry 29*, 4410–4419.
Klemm, J. D., Wozniak, J. A., Alber, T., & Goldenberg, D. P. (1991) *Biochemistry 30*, 589–594.
Kraulis, P. J. (1991) *J. Appl. Crystallogr. 24*, 946–950.
Kuwajima, K., Mitani, M., & Sugai, S. (1989) *J. Mol. Biol. 206*, 547–561.
Oas, T. G., & Kim, P. S. (1988) *Nature 336*, 42–48.
Perry, K. M., Onuffer, J. J., Touchette, N. A., Herridon, C. S., Gittelman, M. S., Matthews, C. R., Chen, J. T., Mayer, R. J., Taira, K., Benkovic, S. J., Howell, E. E., & Kraut, J. (1987) *Biochemistry 26*, 2674–2682.
Sancho, J., Meiering, E. M., & Fersht, A. R. (1991) *J. Mol. Biol. 221*, 1007–1114.
Schwarz, H., Hinz, H. J., Mehlich, A., Tschesche, H., & Wenzel, H. R. (1987) *Biochemistry 26*, 3544–3551.
Segawa, S. I., & Sugihara, M. (1984) *Biopolymers 23*, 2489–98.
Serrano, L., Matouschek, A., & Fersht, A. R. (1992) *J. Mol. Biol. 224*, 805–818.
Shakhnovich, E. I., & Finkelstein, A. V. (1989) *Biopolymers 28*, 1667–1680.
Staley, J. P., & Kim, P. S. (1992) *Proc. Natl. Acad. Sci. U.S.A. 89*, 1519–1523.
Tanford, C. (1968) *Adv. Protein Chem. 23*, 121–282.
van Mierlo, C. P. M., Darby, N. J., Neuhaus, D., & Creighton, T. E. (1991) *J. Mol. Biol. 222*, 373–390.
van Mierlo, C. P. M., Darby, N. J., & Creighton, T. E. (1992) *Proc. Natl. Acad. Sci. U.S.A. 89*, 6775–6779.
van Mierlo, C. P. M., Darby, N. J., Keeler, J., Neuhaus, D., & Creighton, T. E. (1993) *J. Mol. Biol. 229*, 1125–1146.
Weissman, J. S., & Kim, P. S. (1991) *Science 253*, 1386–1393.
Weissman, J. S., & Kim, P. S. (1992) *Proc. Natl. Acad. Sci. U.S.A. 89*, 9900–9904.
Wlodawer, A., Deisenhofer, J., & Huber, R. (1987) *J. Mol. Biol. 193*, 145–156.